Научная статья
Research Article

ОПТИЧЕСКИЙ ЖУРНАЛ. 2023. Том 90. № 9. С. 91–101
OPTICHESKII ZHURNAL. 2023. V. 90. № 9. Pp. 91–101

Оптический журнал
Оптическое приборостроение и метрология
Optical instrument making and metrology

DOI: 10.17586/1023-5086-2023-90-09-91-101
УДК 535.4

Real-time monitoring for composites forming process based on superstructure fiber grating sensing and linear demodulation

Yage Zhan[1]✉, Wenzhuo Zhang[2], Long Xu[3], Min Han[4], Ziting Wang[5]

Donghua University, Shanghai, China

[1]zhanyg@dhu.edu.cn https://orcid.org/0000-0001-9317-3119
[2]2212311@mail.dhu.edu.cn https://orcid.org/0000-0001-9601-683X
[3]2202252@mail.dhu.edu.cn https://orcid.org/0000-0001-6490-3178
[4]2202254@mail.dhu.edu.cn https://orcid.org/0000-0002-5718-9954
[5]928555946@qq.com https://orcid.org/0000-0001-5267-4224

Abstract

Subject of study. An all-fiber grating sensor system has been applied to composites forming monitoring for real-time monitoring of the changes of temperature and strain in the forming process. The **purpose of the work** is optimization of sensor parameters based on fiber-optic Bragg gratings by reducing the effect of photoelectric conversion errors during signal demodulation. **Method.** Two kinds of fiber gratings, including polarization maintaining fiber grating have been used as sensing elements and demodulation elements respectively. The all-fiber sensing system for real-time monitoring of composites forming process has been built. The system acquires the optical signals related to the parameters to be measured, records the optical power of the signal and converts it to the wavelength shift in real time. The temperature and strain can be calculated real-time according to the wavelength. The fiber grating with linear spectrum used as a linear demodulator is designed and developed by ourselves. **Main results.** The demodulator has the linear demodulation in 1544–1556 nm with a linearity of 2.21 dB/nm and the sensor has a dynamic range of 1200 °C and 11000 με. The experimental results show that the all-fiber grating sensor system we designed can clearly reflect the changes of temperature and strain of the composites during the forming process. In the steady state, the maximum temperature difference is less than 10 °C, the maximum temperature difference is less than 100 με, which is consistent with the actual situation. **Practical significance.** The demonstrated feasibility of the sensor system provides a new thought of demodulation and monitoring for composites forming process. Through the further optimization, it can realize more rapid and accurate real-time monitoring for composites forming process.

Keywords: real-time monitoring, superstructure fiber grating, linear demodulation, temperature, strain

Acknowledgment: Supported by Natural Science Foundation of Shanghai (Grant № 21ZR1402400) and Nonlinear Science Institute of Donghua University.

For citation: Zhan Ya., Zhang W., Xu L., Han M., Wang Z. Real-time monitoring for composites forming process based on superstructure fiber grating sensing and linear demodulation [in English] // Opticheskii Zhurnal. 2023. V. 90. № 9. P. 91–101. http://doi.org/10.17586/1023-5086-2023-90-09-91-101

OCIS code: 060.2370

Мониторинг процесса формования композитов с помощью сенсора на основе оптоволоконных брэгговских решеток при использовании линейной демодуляции в реальном времени

Yage Zhan[1]✉, Wenzhuo Zhang[2], Long Xu[3], Min Han[4], Ziting Wang[5]

Donghua University, Shanghai, China

[1]zhanyg@dhu.edu.cn https://orcid.org/0000-0001-9317-3119
[2]2212311@mail.dhu.edu.cn https://orcid.org/0000-0001-9601-683X
[3]2202252@mail.dhu.edu.cn https://orcid.org/0000-0001-6490-3178
[4]2202254@mail.dhu.edu.cn https://orcid.org/0000-0002-5718-9954
[5]928555946@qq.com https://orcid.org/0000-0001-5267-4224

Аннотация

Предмет исследования. Пути проектирования системы сенсоров на оптоволоконных брэгговских решетках для контроля в реальном времени изменений температуры и внутренних силовых напряжений в процессе формирования композитов. **Цель работы.** Оптимизация параметров сенсора на основе оптоволоконных брэгговских решеток посредством уменьшения влияния погрешностей фотоэлектических преобразований при демодуляции сигнала. **Метод.** Экспериментальные исследования оригинальной специально разработанной системы сенсоров контроля температуры и внутренних силовых напряжений в составе двух видов оптоволоконных брэгговских решеток: решетки с усложненной структурой, чувствительной к состоянию поляризации и являющейся источником сигнала, и решетки с линейным спектром, используемой как демодулятор. **Основные результаты.** Практически реализована система сенсоров для контроля изменений температуры и силовых напряжений в процессе формирования композитов с динамическим диапазоном 1200 °C и 11000 МПа и максимальной погрешностью менее 10 °C и 100 МПа соответственно. При этом характеристика демодуляции линейна в диапазоне 1544–1556 нм с линейностью 2,21 дБ/нм. **Практическая значимость.** Подтверждена возможность создания системы сенсоров, обеспечивающей более быстрый и точный мониторинг процесса формования композитов в реальном времени по сравнению с известными системами.

Ключевые слова: мониторинг в реальном времени, оптоволоконный брэгговский сенсор, линейная демодуляция, контроль температуры, внутренние силовые напряжения

Благодарность: работа выполнена при поддержке Фонда естественных наук Шанхая (грант № 21ZR1402400) и Института нелинейных наук Университета Дунхуа.

Ссылка для цитирования: Zhan Ya., Zhang W., Xu L., Han M., Wang Z. Real-time monitoring for composites forming process based on superstructure fiber grating sensing and linear demodulation (Мониторинг процесса формования композитов с помощью сенсора на основе оптоволоконных брэгговских решеток при использовании линейной демодуляции в реальном времени) [на англ. яз.] // Оптический журнал. 2023. Т. 90. № 9. С. 91–101. http://doi.org/10.17586/1023-5086-2023-90-09-91-101

Код OCIS: 060.2370

1. INTRODUCTION

Carbon fiber composites are widely used in aerospace, automobile, high-speed train and other industrial fields due to their high specific strength, corrosion resistance and good designability [1–3]. As the performance of the composites structures is affected by two key forming process parameters, temperature and strain [4, 5], it is necessary to conduct real-time monitoring technology for the two parameters.

Traditional temperature sensors have several defects, such as short service life, unstable performance, slow response and low measurement accuracy. Traditional strain sensors have large volume and are not suitable to be embedded into composites for monitoring [6].

Therefore, optical fiber sensors [7, 8], especially optical fiber grating sensors, have been used for the two parameters' monitoring. Compared with the traditional sensors, optical fiber sensors are small in size and can be embedded into the structures with less influence and good corrosion resistance, electromagnetic interference resistance [9, 10]. At the same time, fiber grating has high sensitivity and resolution with good wavelength coding spectral characteristics [11].

At present, the mode of fiber grating monitoring for composites forming process is based on the characteristics of selecting and reflecting the specific wavelengths [12]. The wavelength is recorded by demodulation instrument, and then the temperature and strain is calculated through data processing [13]. However, this monitoring model has some limitations. This method is easily affected by the photoelectric conversion process, resulting in asynchronous response of collected data and even wavelength data loss. On the other hand, because of the large size of demodulation instrument, it is not convenient to carry, and it is easy to affect the internal optical path structure by vibration in the process of handling, resulting in inaccurate demodulation data.

Therefore, an all-fiber grating sensor has been achieved. Optical fiber gratings, including superstructure fiber grating, are used as the sensing elements and also as demodulation elements. A fiber grating with linear reflection spectrum has been used as the linear demodulator for linear edge filter demodulation. The sensor system can acquire the real-time reflected optical power by the sensing grating and convert the optical power into the wavelength of the grating. The temperature and strain during the composites forming process can be demodulated in real time, which provides a new idea for monitoring the forming process parameters of composites structure.

The purpose of the work is optimization of sensor parameters based on fiber-optic Bragg gratings by reducing the effect of photoelectric conversion errors during signal demodulation.

2. PRINCIPLE

2.1. The sensing principle of embedded fiber Bragg grating

As shown in Fig. 1, the central wavelength λ_B of the reflection spectrum of the fiber Bragg grating (FBG) is mainly modulated by two parameters: the effective refractive index n_{eff} of the fiber core and the periodic length Λ of the grating. The specific relationship is shown as follows:

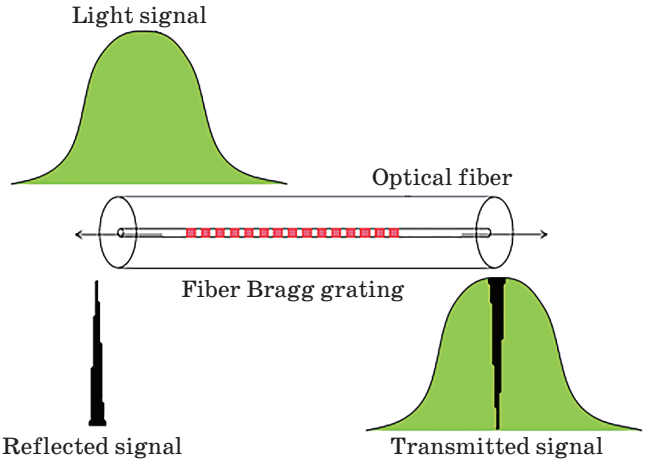

Fig. 1. Fiber Bragg grating sensing principle

Рис. 1. Принцип действия сенсора на основе оптоволоконной брэгговской решетки

$$\lambda_B = 2n_{eff}\Lambda. \quad (1)$$

When the strain and the temperature are applied to the fiber grating, the total wavelength shift can be expressed as

$$\Delta\lambda_{FBG} = \lambda_{FBG}[(1-P_e)\Delta\varepsilon + (\alpha+\xi)\Delta T] = K_\varepsilon\Delta\varepsilon + K_T\Delta T. \quad (2)$$

Here, P_e is the elastic-optic constant, $\Delta\varepsilon$ is the axial strain change, ΔT is the temperature change, K_ε and K_T are respectively the strain coefficient and temperature coefficient, α and ξ are the thermal expansion coefficient and thermo-optic coefficient of optical fiber respectively.

2.2. The sensing principle of polarization maintaining fiber grating

For polarization maintaining fiber Bragg grating (PMFBG), its fast axis and slow axis with stress birefringent have different effective refractive indexes (n_x and n_y). Its reflection spectrum has two reflection peaks with different central wavelengths, as shown in Fig. 2 and expressed by Eqs. (3), (4)

$$\lambda_x = 2n_x\Lambda, \quad (3)$$

$$\lambda_y = 2n_y\Lambda. \quad (4)$$

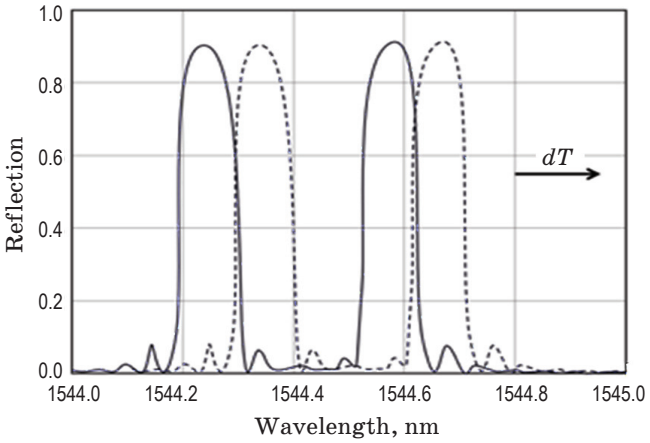

Fig. 2. Reflection signal spectrum of the PMFBG

Рис. 2. Спектр отраженного сигнала оптоволоконной брэгговской решетки со структурой, чувствительной к состоянию поляризации

When its temperature and strain fluctuate, the two wavelengths shift. The shifts of fast axis and slow axis can be expressed by Eqs. (5), (6)

$$\Delta\lambda_x = K_{\varepsilon x}\Delta\varepsilon + K_{Tx}\Delta T, \quad (5)$$

$$\Delta\lambda_y = K_{\varepsilon y}\Delta\varepsilon + K_{Ty}\Delta T. \quad (6)$$

Two formulas can be obtained

$$\Delta\varepsilon = \frac{K_{Tx}\Delta\lambda_y + K_{Ty}\Delta\lambda_x}{K_{\varepsilon y}K_{Tx} + K_{\varepsilon x}K_{Ty}}, \quad (7)$$

$$\Delta T = \frac{K_{\varepsilon x}\Delta\lambda_y + K_{\varepsilon y}\Delta\lambda_x}{K_{\varepsilon x}K_{Ty} + K_{\varepsilon y}K_{Tx}}, \quad (8)$$

where $\Delta\lambda_x$ and $\Delta\lambda_y$ are wavelength shifts of the PMFBG in fast and slow axes, K_{Tx} and K_{Ty} are temperature coefficients in fast and slow axes respectively, $K_{\varepsilon x}$ and $K_{\varepsilon y}$ are strain coefficients of the grating in fast and slow axes respectively.

2.3. Principle of linear filter demodulation

Linear demodulator is based on the principle of edge filtering, which can convert the wavelength shift into the optical power variation within a certain range. When the reflected light of sensor grating enters the linear filter, its output power changes. It needs to convert the optical power into the wavelength shift, so as to realize wavelength demodulation [14].

The output optical power of the linear filter can be expressed as

$$P(\lambda) = K\lambda + B, \quad (9)$$

where k and B are the slope and intercept respectively, which can be measured.

The relation equation $I(\lambda)$ between the reflected light of the grating and the optical power signal can be expressed as follows:

$$I(\lambda) = \int_{-\infty}^{+\infty} R(\lambda - \lambda')H(\lambda')d\lambda'. \quad (10)$$

According to Eq. (10), $H(\lambda)$ and $R(\lambda)$ are the transmission spectral function and grating reflection spectral function of the filter respectively. The approximate linear variation in a smaller norm along its edge can be represented by $I_1(\lambda)$, thus $I(\lambda)$ can be further expressed by $H(\lambda)$ and $I_1(\lambda)$

$$I(\lambda) = H(\lambda)I_1(\lambda), \quad (11)$$

$$I_1(\lambda) = \int_{-\infty}^{+\infty} R(\lambda - \lambda')d\lambda'. \quad (12)$$

According to Formula I_1 and I_2, after the reflected light signal of fiber grating is linearly modulated by matched grating, the reflected peak power changes linearly with wavelength drift. If the linear proportional factor is μ, then

$$V = \mu I(\lambda). \quad (13)$$

When the grating reflected signal passes through the linear filter, the output power of the filter changes, while the reflected signal center wavelength shifts. Therefore, the change of the center wavelength is converted to the change of the optical power, and wavelength demodulation is realized. The method is fast and not affected by photoelectric conversion.

3. EXPERIMENTS

3.1. Schematic diagram of the linear filtering with grating demodulator

The schematic diagram of the linear filtering is shown in Fig. 3. The linear demodulator is a fiber

grating with linear spectrum designed and developed by ourselves. The incident light enters into the sensor grating array through the annular device and forms a narrow band spectrum after the selective reflection. The 3dB coupler divides the light into two beams. I_1 is directly detected to compensate for the influence caused by the fluctuation of the light source. I_2 passes through the linear demodulator and arrives at the photodetector [15].

The specific parameters of the linear demodulator are shown in Table. The reflection spectrum of the linear demodulator is shown in Fig. 4. It can be seen that the linear demodulator has a good linearity in the range of 1544–1556 nm. The conversion between the optical power and the wavelength can be achieved well in this range.

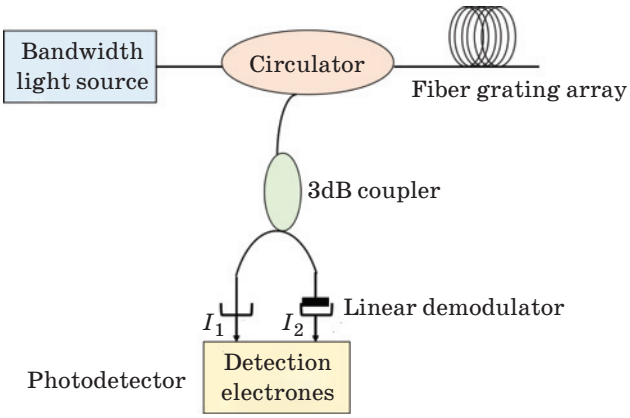

Fig. 3. Schematic diagram of linear demodulator

Рис. 3. Схема линейного демодулятора

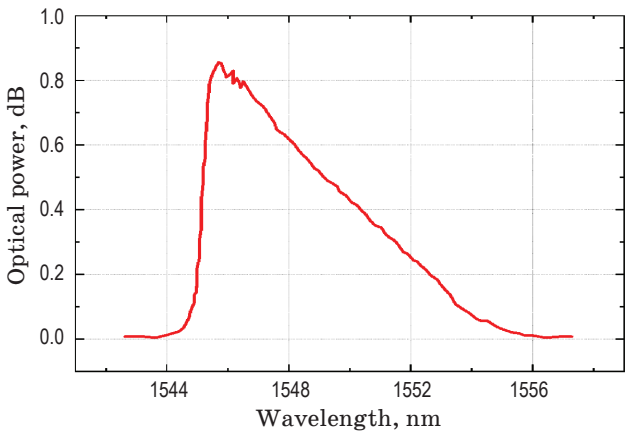

Fig. 4. The reflection spectrum with high performance linear range

Рис. 4. Спектр отраженного сигнала в расширенном диапазоне линейности

Specific parameters of the grating used as linear filter

Параметры решетки, используемой в качестве линейного фильтра

Optical parameters	The numerical
Demodulation range, nm	1544–1556
Transmittance, %	short wavelength 10 long wavelength 90
Bandwidth, nm	12
Linearity rate, dB/nm	2.21

3.2. The validity of the linear demodulator

In order to verify that the designed linear demodulator can respond sensitively to temperature and strain, the experimental systems have been designed as shown in the Fig. 5, and the forming process of composites structures has been monitored.

3.2.1. The schematic diagram of the sensor with linear demodulator

Figure 5 shows the schematic diagram of the sensor system with linear demodulator. Wavelength acquisition is carried out by the grating linear demodulator and by high-speed demodulator MOI[1] for comparison.

For verification and comparison, the laying scheme of the sensor grating is designed. A total of 10 layers of composites pre-preg laminates were laid in the experiment. Four FBGs were laid at different angles on the fifth layer, as shown in Fig. 6.

3.2.2. Results of the linear demodulator verification

FBG1, FBG2, and FBG3 are connected to channel 1, channel 2, and channel 3 of the demodulation instrument respectively. FBG4 is connected to the linear filter, and its reflection optical power can be converted to its wavelength shift. The wavelength shifts of the four sensor gratings are plotted together, as shown in Fig. 7.

It can be seen from Fig. 7 that time interval 0–40 min is the heating stage, and the resin flow releases a lot of heat, so the slope of the curve is large. Time interval 40–140 min is the insulation stage, the oven is close to the set temperature, so the curve rises gently. Close the oven for natural

[1] Micron Optics Int.

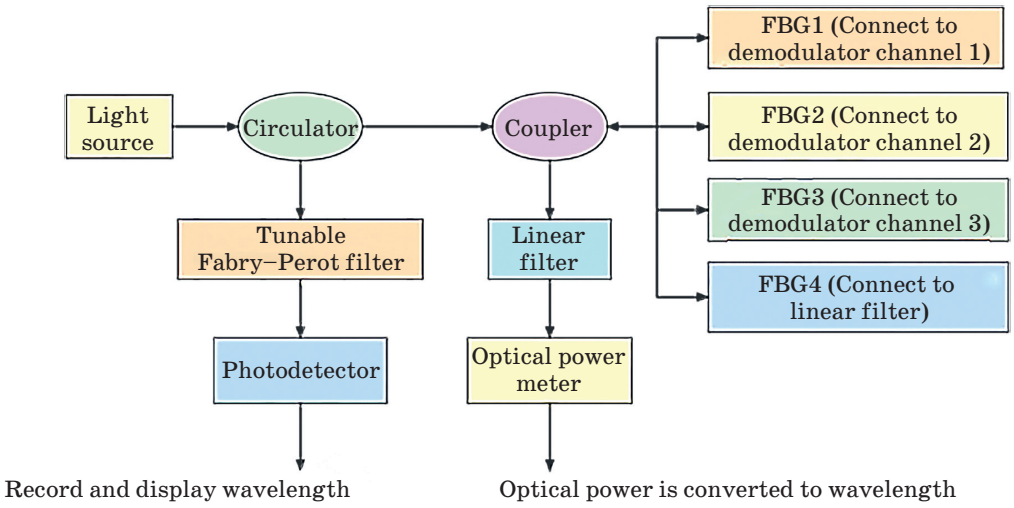

Fig. 5. The schematic diagram of the monitoring system for verification and comparison

Рис. 5. Структурная схема системы мониторинга для ее экспериментальной проверки

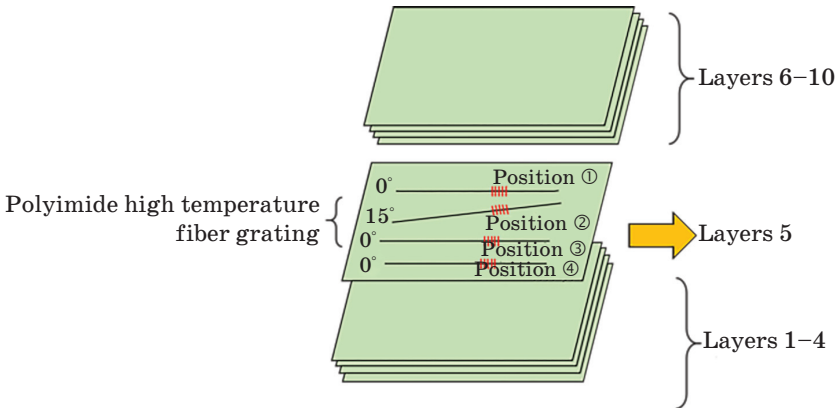

Fig. 6. The laying scheme for validation experiment (FBG1 at position ①, FBG2 at ②, FBG3 at ③, and FBG4 at ④)

Рис. 6. Схема уровней при экспериментальной проверке (FBG1 в позиции ①, FBG2 — ②, FBG3 — ③, and FBG4 — ④)

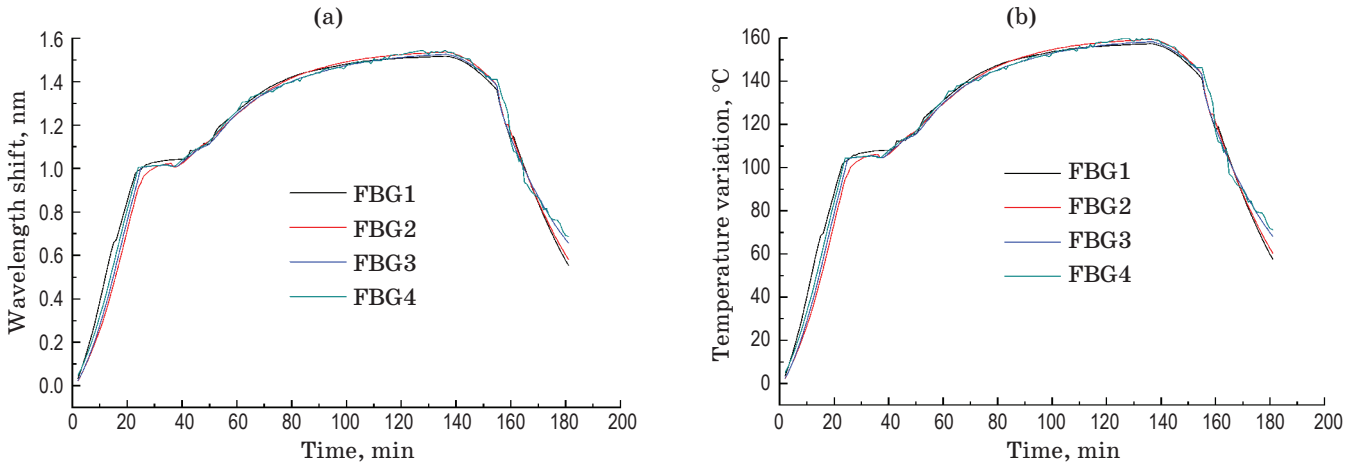

Fig. 7. (a) Wavelength shift and (b) temperature variation of validation experiment

Рис. 7. Смещение длины волны (а) и изменение температуры (б) при экспериментальной проверке

cooling after 140 min. Due to the large temperature difference between inside and outside the oven, the rapid drop of temperature leads to the shrinkage of the resin inside the material, and the curve shows the large slope decline.

The wavelength shift of FBG1, FBG2, and FBG3 in the figure can well reflect the macro changes of the composites forming process, and the results of the three sensors are consistent, which demonstrates the accuracy of the instrument monitoring, and provides a reliable reference for the comparison of the designed linear demodulator.

During the heating stage, the linear modem demodulating wavelength and demodulating wavelength demodulation apparatus have a certain error, this is due to the unstable temperature change inside the oven. In other stages, the temperature measured by the linear demodulator is consistent with the temperature measured by the other three high precision demodulators, which proves that the designed linear filter has a good feasibility.

3.3. The all-fiber grating sensor

In Section 3.2, the effectiveness of the designed linear demodulator is verified. In this section, an all-fiber grating sensor is achieved based on the linear demodulator. The all-fiber grating sensor uses fiber gratings as both sensing elements and demodulators, which eliminates the influence of photoelectric conversion and provides a new idea for composites forming monitoring.

3.3.1. The diagram of the all-fiber grating sensor

In the all-fiber grating sensor system, the FBG and the PMFBG are used as the sensing element, and the linear demodulator is used for demodulation, as shown in Fig. 8. The temperature and strain can be demodulated by recording the optical power with the linear demodulator according to the relationship between the optical power.

3.3.2. Laying scheme of the gratings for the experiments with all-fiber system

In the experiment, a total of 10 layers of composites pre-preg laminates were laid. Two FBGs and one PMFBG were laid on the fifth layer to ensure that the gratings were in the center of the laminates. Keeping the three gratings close to each other ensures that temperature and strain are evenly distributed during the forming process, as shown in Fig. 9.

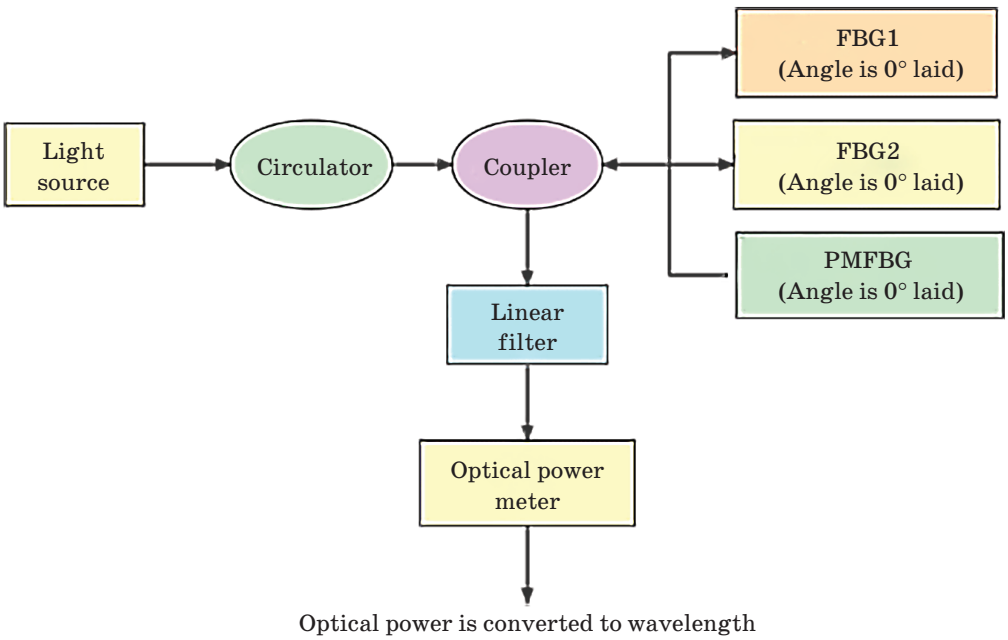

Fig. 8. The schematic diagram of the all-fiber sensor system

Рис. 8. Структурная схема системы сенсоров

4. RESULTS AND ANALYSIS

According to the laying scheme in Fig. 9, the composites forming process is monitored, and the temperature and strain are demodulated by linear demodulator, so as to realize the online monitoring of the all-fiber sensor system.

Figure 10a shows the temperature results. The curve can well reflect the heating, insulation and cooling stages of the process. The thermocouple can withstand the temperature of about 250 °C and is stable at about 180 °C, so that it can provide a reliable reference for verifying the accuracy of the all-fiber grating sensor.

In the heating stage, the maximum difference of the monitored temperature between FBG, PMFBG and thermocouple is 1.5 and 3 °C respectively. The main reason may be the instability of temperature change and the inconsistency of heating at different positions inside the material. However, with the increase of time, the difference gradually decreases after the heating stage tends to be stable.

In the insulation stage, the maximum difference of the monitored temperature between FBG, PMFBG and thermocouple is 1.8 and 2 °C respectively. This difference is mainly caused by the inconsistency of heat release caused by the flow rate of resin at different positions inside the material.

In the cooling stage, the maximum difference of the monitored temperature between FBG, PMFBG and thermocouple is 2 and 3 °C respectively. At the last stage of the cooling process, the slope of PMFBG is smaller than the FBG and thermocouple; this is because the cooling in this position is faster and the completion of curing is earlier than in other positions.

In the process of composite molding, the process conditions are set as heating stage – constant temperature stage – slow cooling stage – fast cooling stage. As can be seen from Fig. 10a, during time interval 0–70 min, the temperature monitored by the three sensors presents an almost linear rise. In time interval 70–115 min, the temperature is always in a constant state of 180 °C; since the set temperature of oven is 160 °C, the temperature drops almost linearly. At 140 min, the oven is turned off and the temperature drops rapidly. In conclusion, the temperature monitored by the sensor meets the set process conditions.

In order to verify the effectiveness of the all-fiber sensor system, two repeated experiments were carried out. A FBG was used as the sensing element, and the temperature changes during the experiment were demodulated. Meanwhile, the temperature measured by thermocouple was compared as shown in Figs. 10c, d.

It can be seen from Figs. 10c, d that the temperature monitored by the all-fiber sensor system has basically the same trend as that monitored by the thermocouple in different experiments, and the monitoring results can reflect the temperature that changes dynamically during the forming process of thermoplastic composites. Compared to the thermocouple, the FBG monitoring of the temperature fluctuation is more obvious, so the curve is not smooth; this is because the FBG is more sensitive to the temperature changes, even the tiny temperature

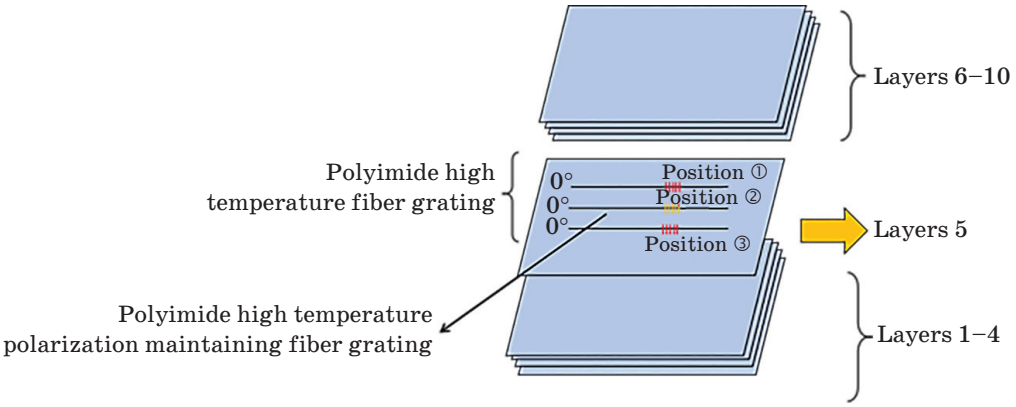

Fig. 9. The laying scheme for all-fiber grating sensor (FBG1 at position ①, FBG2 at ②, PMFBG at ③)

Рис. 9. Схема уровней системы оптоволоконных сенсоров на основе брэгговских решеток (FBG1 в позиции ①, FBG2 — ②, PMFBG — ③)

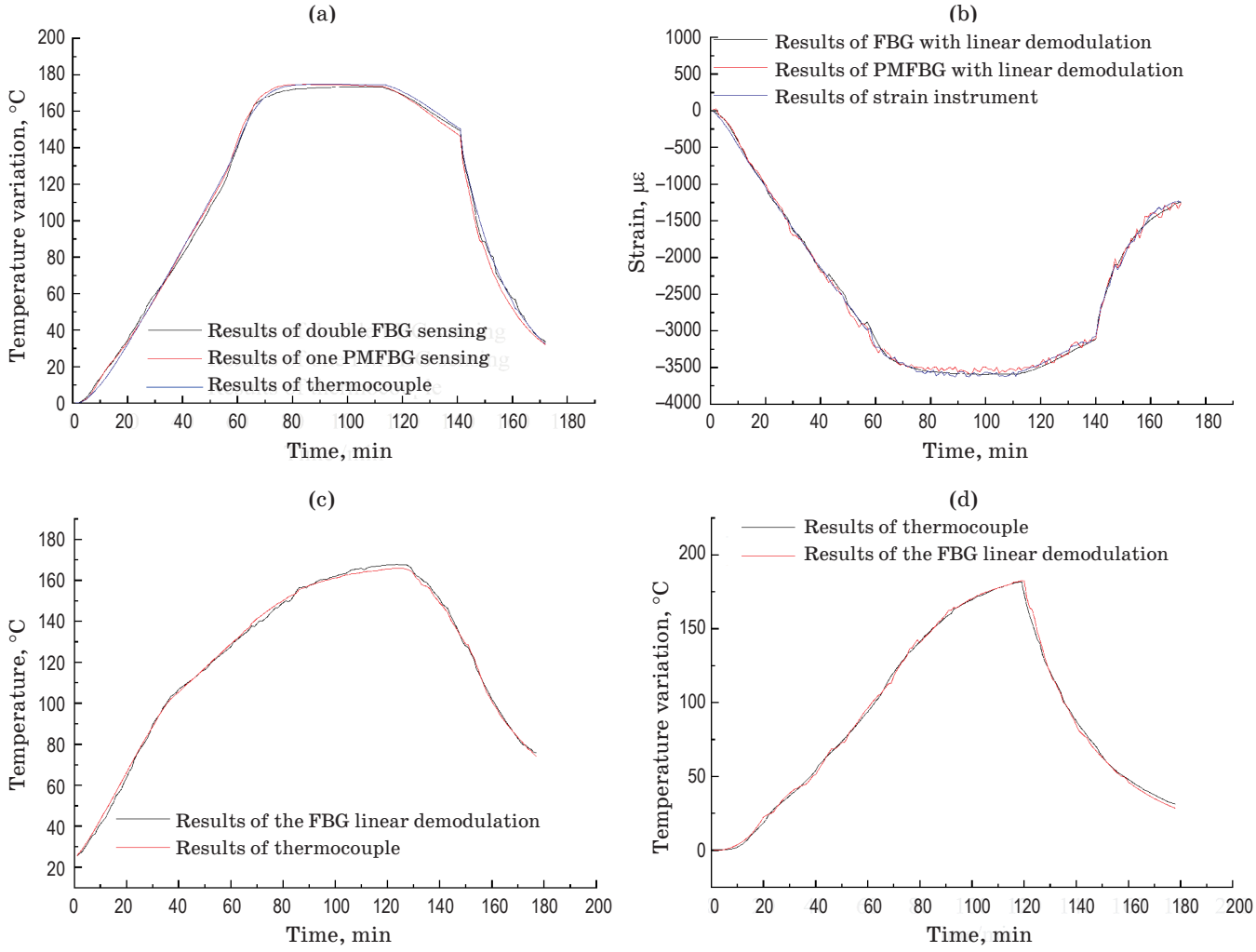

Fig. 10. (a) Temperature variations and (b) strain results of the all-fiber grating sensor. (c) Temperatures of validation in the 1st and (d) 2nd experiments

Рис. 10. Температурные изменения (a) и результаты измерения внутренних напряжений (b) системой оптоволоконных сенсоров на основе брэгговских решеток. Результаты измерения температуры в первом (c) и втором (d) экспериментах

changes can cause Bragg wavelength shift, which can reflect the complex changes of the composites forming process in more realistic light.

In the repeated experiments, the process conditions were set as heating stage — cooling stage. As can be seen from Fig. 10c, the temperature monitored by grating and thermocouple increases during time interval 0–130 min. After 130 min, the oven temperature is set at 80 °C, and it can be seen that the temperature drops almost linearly and slowly. It can be seen from Fig. 10d that the temperature rises during time interval 0–120 min. At 120 min, the oven is turned off and the temperature drops rapidly.

In order to test the strain monitoring ability of the full grating demodulation system, a comparative analysis was made between the strain monitored by the all-fiber system and that one directly measured by the strain gauge, as shown in Fig. 10b. The three curves can well reflect the heating, insulation and cooling stages of the composites forming process, and the curve trend is basically the same.

During the heating stage, the thermal expansion effect is produced by the release of large amounts of heat from resin melting, so the strain increases. After 20 min of the heating stage, the maximum difference of ε_{FBG}, ε_{PMFBG} and strain gauge is about 200 με. The main reason

may be the different degree of thermal expansion effect at different positions in the material. In the insulation stage, the oven stops heating up, and the internal strain changes of the material tend to be stable. The strain monitored by the three sensors fluctuates around 3500 με. After 90 min, it enters the cooling stage. At this time, the strain is greatly affected by the temperature, and the temperature difference between inside and outside the oven is used for rapid heat exchange, and the resin inside the material shrinks, when it is cold. Resin flow velocity and gel point time are different at different locations, leading to certain differences in strain in cooling stage compared with heating and insulation stages.

5. CONCLUSIONS

In this paper, we designed and developed the fiber grating linear demodulator based on the edge filter demodulation principle and applied it for the monitoring of composites forming process. Firstly, the verification experiments have been accomplished. The feasibility and effectiveness of the linear demodulator have been proved. The experimental results have been compared to those obtained by the high-precision MOI demodulator. It has been proved that the linear demodulator can clearly reflect the heating stage, insulation stage, and cooling stage of the composites forming process. The demodulator range is 1544–1556 nm, and the bandwidth is 12 nm. The wave-power linearity is 2.21 dB/nm.

Secondly, by combining the designed linear demodulator with the FBG and the PMFBG, the all-fiber sensor system was built. The fiber grating was used as both the sensing element and demodulation element, which reduced the influence of the photoelectric conversion in the traditional demodulation method. The feasibility of the all-fiber grating sensor has been verified by applying it to the monitoring of the composites forming process. The experimental results show that the all-fiber grating sensor can directly monitor the temperature and strain of the composites during the forming process. In the steady state, the maximum temperature difference is less than 10 °C, the maximum temperature difference is less than 100 με, which is consistent with the actual situation.

In conclusion, the all-fiber grating sensor has been applied to composites forming monitoring. The demonstrated feasibility of the sensor system provides a new thought of demodulation and monitoring for composites forming process. Through the further optimization, it can realize more rapid and accurate real-time monitoring for composites forming process.

REFERENCES

1. Ma Q., Li J., Tian S. Forming technology of thermoplastic composite and its application in aircraft // New Chem. Mater. 2022. V. 50. № 6. P. 263–266, 271.
2. Roux M., Eguemann N., Dransfeld C., et al. Thermoplastic carbon fibre-reinforced polymer recycling with electrodynamical fragmentation: From cradle to cradle // J. Thermoplastic Composite Mat. 2017. V. 30. № 3. P. 381–403. https://doi.org/10.1177/0892705715599431
3. Avci H., Akkulak E., Gergeroglu H., et al. Flexible poly(styrene-ethylene-butadiene-styrene) hybrid nanofibers for bioengineering and water filtration applications // J. Appl. Polymer Sci. 2020. V. 137. № 26. P. 49184. https://doi.org/10.1002/app.49184
4. Wang C.T., Hsieh T.S., Hsu H.C., et al. Curing monitoring of cross-ply and quasi-isotropic-ply carbon fiber/epoxy composite material with metal-coated fiber Bragg grating sensors // Optik. 2019. V. 184. P. 490–498. https://doi.org/10.1016/j.ijleo.2019.04.126
5. Chen J., Fu K., Li Y. Understanding processing parameter effects for carbon fibre reinforced thermoplastic composites manufactured by laser-assisted automated fibre placement (AFP) // Composites Part a-Appl. Sci. and Manufacturing. 2021. V. 140. P. 160. https://doi.org/10.1016/j.compositesa.2020.106160
6. Zhan Y., Lin F., Guo A., et al. Polyimide-coated fiber Bragg grating sensor for monitoring of the composite materials curing process // J. Opt. Technol. 2020. V. 87. № 8. P. 501–505. https://doi.org/10.1364/jot.87.000501
   Zhan Y., Lin F., Guo A. и др. Датчик для мониторинга процессов технологической обработки композитных материалов, использующий брэгговскую решётку в волокне с полиимидной оболочкой [in English] // Оптический журнал. 2020. Т. 87. № 8. С. 72–78. https://doi.org/10.17586/1023-5086-2020-87-08-72-78
7. Nascimento M., Inacio P., Paixao T., et al. Embedded fiber sensors to monitor temperature and strain of polymeric parts fabricated by additive manufacturing and reinforced with NiTi wires // Sensors. 2020. V. 20. № 4. P. 1122. https://doi.org/10.3390/s20041122
8. Tsukada T., Minakuchi S., Takeda N. Identification of process-induced residual stress/strain distribution in thick thermoplastic composites based on in situ strain monitoring using optical fiber sensors // J. Composite Mat. 2019. V. 53. № 24. P. 3445–3458. https://doi.org/10.1177/0021998319837199
9. Konstantaki M., Violakis G., Pappas G.A., et al. Monitoring of torque induced strain in composite shafts with embedded and surface-mounted optical fiber

Bragg gratings // Sensors. 2021. V. 21. № 7. P. 2403. https://doi.org/10.3390/s21072403
10. Zhang J., Yu H., Li L., et al. Study of monitoring CF3052/5224 composites molding process by optical fiber Bragg grating // Mat. Sci. and Technol. 2015. V. 23. № 4. P. 17–22. http://dx.doi.org/10.11951/j.issn.1005-0299.20150403
11. Hsiao T.C., Hsieh T.S., Chen Y.C., et al. Metal-coated fiber Bragg grating for dynamic temperature sensor // Optik. 2016. V. 127. № 22. P. 10740–10745. https://doi.org/10.1016/j.ijleo.2016.08.110
12. Wang J., Zhu W., Ma C., et al. FBG wavelength demodulation based on a radio frequency optical true time delay method // Opt. Lett. 2018. V. 43. № 11. P. 2664–2667. https://doi.org/10.1364/ol.43.002664
13. Bloessl Y., Hegedus G., Szebenyi G., et al. Applicability of fiber Bragg grating sensors for cure monitoring in resin transfer molding processes // J. Reinforced Plastics and Composites. 2021. V. 40. № 19–20. P. 701–713. https://doi.org/10.1177/0731684420958111
14. Melle S.M., Liu K.X., Measures R.M. A passive wavelength demodulation system for guided-wave Bragg grating sensors // IEEE Photon. Technol. Lett. 1992. V. 4. № 5. P. 516–518. https://doi.org/10.1109/68.136506
15. Wu J., Wu H., Huang J., et al. Research progress in edge filter demodulation method of fiber Bragg grating sensors // Opt. Commun. Technol. 2014. V. 38. № 4. P. 38–41. https://doi.org/10.1364/OE.433914

AUTHORS

Yage Zhan — Doctor of Engineering, Professor, Donghua University, Shanghai, 201620, China; Scopus ID: 7102619897; https://orcid.org/0000-0001-9317-3119; zhanyg@dhu.edu.cn

Wenzhuo Zhang — Student, Donghua University, Shanghai, 201620, China; https://orcid.org/0000-0001-9601-683X; 2212311@mail.dhu.edu.cn

Long Xu — Student, Donghua University, Shanghai, 201620, China; https://orcid.org/0000-0001-6490-3178; 2202252@mail.dhu.edu.cn

Min Han — Student, Donghua University, Shanghai, 201620, China; https://orcid.org/0000-0002-5718-9954; 2202254@mail.dhu.edu.cn

Ziting Wang — Student, Donghua University, Shanghai, 201620, China; https://orcid.org/0000-0001-5267-4224; 928555946@qq.com

The article was submitted to the editorial office 10.11.2022
Approved after review 05.12.2022
Accepted for publication 24.07.2023

Статья поступила в редакцию 10.11.2022
Одобрена после рецензирования 05.12.2022
Принята к печати 24.07.2023